

# A METHOD OF FINGERPRINT IMAGE ENHANCEMENT BASED ON SECOND DIRECTIONAL DERIVATIVES

Marius Tico, Markku Vehvilainen, Jukka Saarinen

Nokia Research Center, POBox 100, FIN-33721 Tampere, Finland

## ABSTRACT

We present an approach to fingerprint image enhancement that relies on detecting the fingerprint ridges based on the sign of the second directional derivative of the digital image. A facet model is used in order to approximate the derivatives at each image pixel based on the intensity values of pixels located in a certain neighborhood. The size of this neighborhood determines the scale of the image details that are preserved. We develop a selection criterion for the neighborhood size that aims to preserve minutiae details and remove smaller details from the enhanced image. The experimental results demonstrate the ability of the proposed approach to preserve a large percent of the genuine minutiae in the enhanced image.

## 1. INTRODUCTION

Fingerprints are graphical ridge patterns present on human fingers, which, due to their uniqueness and permanence, are among the most reliable human characteristics that can be used for people identification [1]. A common hypothesis, confirmed by the experience accumulated during a century of forensic use of fingerprints, is that certain local structures derived from the fingerprint ridges, called minutiae, are able to capture the invariant and discriminatory information present in the fingerprint image.

Several factors like the presence of scars, variations of the pressure between the finger and acquisition sensor, worn artifacts, the environmental conditions during the acquisition process, etc., can dramatically affect the quality of the acquired fingerprint image. Since minutiae depend on fine details of the ridge pattern, their extraction can become notoriously difficult if the “noise” generated by the factors described above is not substantially reduced. The main goals of a fingerprint image enhancement algorithm are: (i) to reduce the noise present in the image, and (ii) to detect the fingerprint ridges. An input gray-scale fingerprint image is thereby transformed by the enhancement algorithm into a binary representation of the ridge pattern, called binary ridge-map image.

In the method proposed by Ratha, *et al.* in [2] the image is smoothed using a one-dimensional averaging mask oriented along the local ridge orientation, and the fingerprint ridges are detected as local minima of the gray level projection waveform along a scan line perpendicular to the local ridge orientation. Jain, *et al.* [3] proposed to accentuate local minima intensity values along a direction normal to the local ridge orientation by convolving the fingerprint image with two masks aligned to the ridge orientation. Subsequently, a binary ridge-map image is obtained by comparing the intensity values of the pixels in the two convolved images with a certain threshold value. Sherlock, *et al.* [4] proposed a directional Fourier domain filtering for fingerprint enhancement. They design a set of 16 directional filters tuned on different orientations

between 0 and  $\pi$ . Applying each filter onto the entire fingerprint image they obtain 16 filtered images. Next, the value of each pixel in the enhanced image is selected from one of the 16 filtered images based on the ridge orientation in the neighborhood of that pixel. Instead of designing filters tuned on corresponding spatial frequency of each image region Willis and Myers proposed in [5] to use as filter directly the magnitude of the Fourier transform of the local image region. This magnitude already exhibits most of the qualities required from a properly designed enhancement filter since it has a dominant component at the corresponding ridge orientation and frequency, and on the other hand, due to the noise irregularity it exhibits small other components.

The fingerprint image enhancement approach, proposed in this paper, relies on the sign of the second direction derivative of the image intensity surface. The image curvature is calculated in each pixel along the direction orthogonal to the local ridge orientation, following then to assign the pixels of positive curvature to the ridges. A polynomial facet model is used to estimate the derivatives of the discrete intensity surface of the image. According to this model, the image curvature in each pixel is calculated based on the intensity levels of several pixels located in a certain neighborhood window of the pixel of interest. The size of this neighborhood determines the size of image details that are preserved after the operation. We propose a selection criterion for this neighborhood size that ensures the preservation of minutiae features, removing smaller image details that may generate false minutiae.

## 2. ESTIMATION OF IMAGE CURVATURE

A fingerprint image exhibits a quasi-periodic structure of alternating ridge and valley tracks. A cross section through several ridges exhibits an almost sinusoidal profile of the gray level intensity, where low (high) values correspond to pixels situated on ridges (valleys). The discrimination between ridge and valley pixels can be performed based on the sign of the second derivative of such one dimensional sequence of intensity levels, the positive (negative) values of this derivative corresponding to ridges (valleys). Based on this observation, we propose to detect the fingerprint ridges in those image pixels where the second directional derivative along the direction orthogonal to the local ridge orientation is positive.

Let  $g(i, j)$  denotes the value of the gray-level intensity in the pixel  $(i, j)$  of the image, where  $i$  denotes the horizontal coordinate that increases from left to right, and  $j$  denotes the vertical coordinate that increases from bottom to up. Also, let  $\theta \in [0, \pi)$  denotes the local ridge orientation with respect to the horizontal axis. The second derivative of the intensity surface along the direction  $\mathbf{v} = [-\sin \theta \ \cos \theta]^T$ , orthogonal to the local ridge orientation is

given by

$$\begin{aligned} g''_{\mathbf{v}}(i, j) &= g^{(2,0)}(i, j) \sin^2 \theta \\ &+ g^{(0,2)}(i, j) \cos^2 \theta \\ &- g^{(1,1)}(i, j) \sin 2\theta, \end{aligned} \quad (1)$$

where  $g^{(p,q)}(i, j)$  denotes the  $(p + q)$ th partial derivative of the discrete intensity surface at site  $(i, j)$ ,  $p$  along the horizontal axis and  $q$  along the vertical axis.

The second partial derivatives of the discrete intensity surface can be approximated using a facet model [6]. This consists of estimating a continuous and differentiable surface (facet) that fits over the gray levels of the image pixels located in a neighborhood of  $(i, j)$ , following then to approximate the image derivatives in  $(i, j)$  with the derivatives of this surface. Using a separable parametric model for the facet [7, 8], we obtain the approximation of the  $(p, q)$  derivative

$$g^{(p,q)}(i, j) \approx \sum_{c, r=-L}^L \mathbf{f}_{p,L}(c) \mathbf{f}_{q,L}(r) g(i-c, j-r), \quad (2)$$

where  $\mathbf{f}_{p,L}$  and  $\mathbf{f}_{q,L}$  are the impulse responses of 1D FIR filters of length  $2L+1$ , that act along the image rows and columns. A useful property is that the filter coefficients do not depend on image data. Consequently, they can be computed beforehand based solely on the parametric model chosen for the facet. As an example, using a 3rd order polynomial facet model, one can derive the following formulas for the filter coefficients

$$\begin{aligned} \mathbf{f}_{0,L}(\ell) &= \frac{3(3L^2 + 3L - 1 - 5\ell^2)}{(2L+1)(2L-1)(2L+3)}, \\ \mathbf{f}_{1,L}(\ell) &= \frac{[-5\ell(15L^4 + 30L^3 - 15L + 5 - 21L^2\ell^2 - 21L\ell^2 + 7\ell^2)]/[L(L+1)(2L+1) \times (L-1)(2L-1)(L+2)(2L+3)]}{30(3\ell^2 - L^2 - L)}, \\ \mathbf{f}_{2,L}(\ell) &= \frac{30(3\ell^2 - L^2 - L)}{L(L+1)(2L+1)(2L-1)(2L+3)}. \end{aligned} \quad (3)$$

### 3. SELECTION OF THE APPROXIMATION ACCURACY

Maintaining a fixed parametric model for the facet, we can choose the size of the approximation neighborhood around each pixel in order to adjust the approximation accuracy. The smaller the neighborhood size the better the approximation of the discrete intensity levels of image pixels. Our goal is to select the size of the approximation neighborhood (or similarly the approximation accuracy), such that to ensure the preservation of genuine minutiae details, and the deletion of smaller image details that may generate false minutia. In this section we develop a criterion that can be used to select the best size of the approximation neighborhood (i.e.  $(2L+1) \times (2L+1)$ ), among certain given candidates.

Noting that the minutiae details are features that have sizes comparable with the ridge period, we approach the problem of selecting the best neighborhood size indirectly, by developing first an estimator of the ridge period based on second directional derivative of the digital image. The accuracy of the proposed estimator depends of the approximation neighborhood size. Accurate estimates being obtained for those values of  $L$  which preserve details of the same size as the ridge period and remove much smaller details.

Consequently, the variance of the proposed ridge period estimator will be used to construct the neighborhood size selection criterion.

In the absence of noise, we may consider that the gray level intensities along the orthogonal direction to the ridge orientation are samples of the continuous function

$$f(x) = A \cos\left(\frac{2\pi}{\tau_{in}}x + \Phi\right) + B, \quad (4)$$

where  $\tau_{in}$  denotes the local ridge period expressed in inch. The constant factor  $B$  stands for the local average gray level intensity, and  $A$  and  $\Phi$  denote respectively the amplitude and the phase of the sinusoidal wave.

Using the second derivative of (4) one can determine the ridge period by noting that

$$\tau_{in} = 2\pi \left[ -\frac{f(x) - B}{f''(x)} \right]^{1/2}, \quad (5)$$

for any  $x$  where  $f''(x) \neq 0$ .

A discrete signal  $g(n) = f(nT)$ , is obtained by sampling the sinusoidal wave (4). The sampling period  $T$  depends on the resolution used for image acquisition; for instance  $T = 0.002$  inch if the image is acquired at a resolution of 500 dots per inch. The discrete signal can be written as

$$g(n) = A \cos\left(\frac{2\pi}{\tau}n + \Phi\right) + B, \quad (6)$$

where  $\tau = \tau_{in}/T$  denotes the ridge period expressed in number of pixels. Next, the second derivative of the discrete signal can be approximated using, for instance, the filter  $\mathbf{f}_{2,L}$  from (3)

$$\begin{aligned} g''(n) &= \sum_{\ell=-L}^L \mathbf{f}_{2,L}(\ell) g(n-\ell) \\ &= \left[ \sum_{\ell=-L}^L \mathbf{f}_{2,L}(\ell) \cos\left(\frac{2\pi}{\tau}\ell\right) \right] A \cos\left(\frac{2\pi}{\tau}n + \Phi\right), \end{aligned} \quad (7)$$

where we used the properties  $\sum_{\ell=-L}^L \mathbf{f}_{2,L}(\ell) = 0$ , and  $\mathbf{f}_{2,L}(\ell) = \mathbf{f}_{2,L}(-\ell)$ , for any integer  $\ell \in [-L, L]$ .

It is clear that in the discrete case we cannot determine the ridge period as simple as in the continuous case. Nevertheless, the ratio on the right hand side of (5) is still useful since it eliminates the nuisance parameters  $A$ , and  $\Phi$ . Therefore, given the discrete signal  $g(n)$  and its second derivative  $g''(n)$ , we can calculate first the value

$$\Gamma = -[g(n) - B]/g''(n), \quad (8)$$

for any  $n$  where  $g''(n) \neq 0$ , following then to determine  $\tau$  as the solution of the equation

$$\sum_{\ell=-L}^L \mathbf{f}_{2,L}(\ell) \cos\left(\frac{2\pi}{\tau}\ell\right) = -\frac{1}{\Gamma}. \quad (9)$$

Unfortunately, equation (9) is difficult to solve analytically, except for the particular case when the ridge period is relatively large in comparison with the length of the filter  $\mathbf{f}_{2,L}$ . In such a case, using the first two terms of the Taylor series approximation for the cosine function, we have that  $\tau \approx 2\pi\sqrt{\Gamma}$ .

In general however, this Taylor series approximation does not stand, and hence we adopted a table lookup based solution. Noting

that  $\Gamma$  is a monotonically increasing function of  $\tau$  (for  $\tau \geq 2L$ ), and that the ridge period is typically between 3 and 20 pixels, we calculate beforehand the values of  $\Gamma$  at  $\tau \in \{3, 4, \dots, 20\}$  and store them in a lookup table. Subsequently, for a given  $\Gamma$  the value of the ridge period ( $\tau$ ) stored in the nearest entry is delivered.

Until now we introduced the theoretical framework of our approach. For simplicity, we assumed an ideal sinusoidal model of the ridge profile in the absence of noise, and hence the parameter  $\Gamma$  took the same value at all  $n$  where  $g''(n) \neq 0$ . In practice, because the ridge profile is not a perfect sinusoid, as well as because of the presence of noise, we must estimate  $\Gamma$  from its observed values at different samples  $n$ . The value of  $\Gamma$  observed at the  $n$ -th sample ( $g''(n) \neq 0$ ) is given by

$$\gamma_n = -\frac{g(n) - \bar{g}}{g''(n)}, \quad (10)$$

where  $\bar{g}$  denotes the sample average of the observed data.

We assume that the  $N$  observed values of  $\Gamma$  are corrupted by an independent identically distributed noise  $\eta_n$

$$\gamma_n = \Gamma + \eta_n, \quad 1 \leq n \leq N, \quad (11)$$

whose distribution is approximated by Laplacian distribution (see Fig. 1).

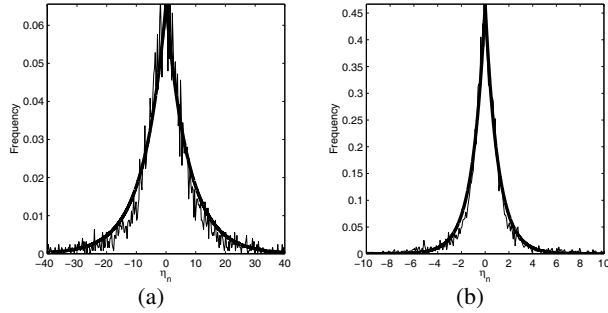


**Fig. 1.** The estimated p.d.f. of  $\eta_n$  (thin line), and the theoretical Laplacian p.d.f. (thick line). Both figures have been constructed based on 5000 samples of a unity amplitude sinusoidal wave in Gaussian noise of variance 0.5. The period of the sinusoidal wave was 10 in (a), and 4 in (b), and the size of the filters used were  $L = 5$  in (a), and  $L = 2$  in (b).

Consequently, the maximum likelihood (ML) estimate of  $\Gamma$  is the median of the  $N$  observed values

$$\hat{\Gamma} = \text{median}\{\gamma_1, \gamma_2, \dots, \gamma_N\}, \quad (12)$$

and the ML estimate of noise variance is given by

$$\text{var}(\eta_n) = 2 \left[ \frac{1}{N} \sum_{n=1}^N |\gamma_n - \Gamma| \right]^2. \quad (13)$$

Let us now make some considerations about the approximation of the second directional derivative (1). This formula, carried out for all samples of the discrete signal  $g$ , is equivalent with a convolution between the signal and a certain 2D FIR filter. The size of this filter (i.e.,  $(2L+1) \times (2L+1)$ ) must be selected in accordance to the ridge period in order to obtain an accurate estimate

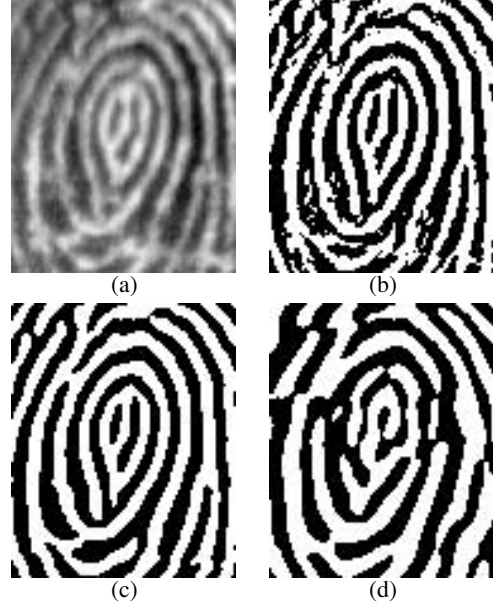


**Fig. 2.** Enhancement results and criterion values obtained with different filter sizes: (a) original image, (b)  $L = 2$ ,  $C = 4.3$ , (c)  $L = 4$ ,  $C = 0.8$ , and (d)  $L = 8$ ,  $C = 1.3$ .

of the parameter  $\Gamma$ , and hence an accurate estimate of the ridge period. To break this vicious circle, we note that the variance (13) can be used as an indicator of the accuracy achieved in estimating  $\Gamma$ . However, because filters of different sizes have different energy values, denoted here by  $e(L)$ , the variance (13) must be also normalized accordingly in order to serve as a selection criterion for the filter size. Alternatively, the filters (3) could be divided to their Euclidean norm before usage, in which case  $e(L) \approx 1$ .

Let  $L_1 < L_2 < \dots < L_K$  denote  $K$  preselected values of the parameter  $L$ , each of them being used to design a certain set of filters (3). Applying these filters onto the given signal we obtain  $K$  different approximations of  $g''$ , and hence  $K$  different sets of observations (10). Let  $\{\gamma_n^{(k)}; 1 \leq n \leq N\}$  denotes the set of observations obtained using a filter of length  $2L_k + 1$ , and  $\hat{\Gamma}^{(k)}$  denotes the estimated value of parameter  $\Gamma$  in this case. The selection criterion that we propose to minimize in order to select an appropriate filter size is

$$C_k = \frac{e(L_k)}{N} \sum_{n=1}^N |\gamma_n^{(k)} - \hat{\Gamma}^{(k)}|. \quad (14)$$

#### 4. EXPERIMENTAL RESULTS

Enhancement results, achieved with filters of different sizes, are exemplified in Fig.2. Visually, the most accurate ridge segmentation result is obtained for  $L = 4$ , shown in Fig. 2(c). We note that this is also well indicated by the value of the proposed criterion (14), which is smaller in (c) than in the (b) and (d) cases of Fig. 2.

In the following experiments we employed a fingerprint enhancement algorithm based on  $K = 4$  triplets of filters (3), designed for  $L \in \{2, 3, 4, 5\}$ . The algorithm calculates  $K$  candidate directional curvature images for a fingerprint. Next, it constructs

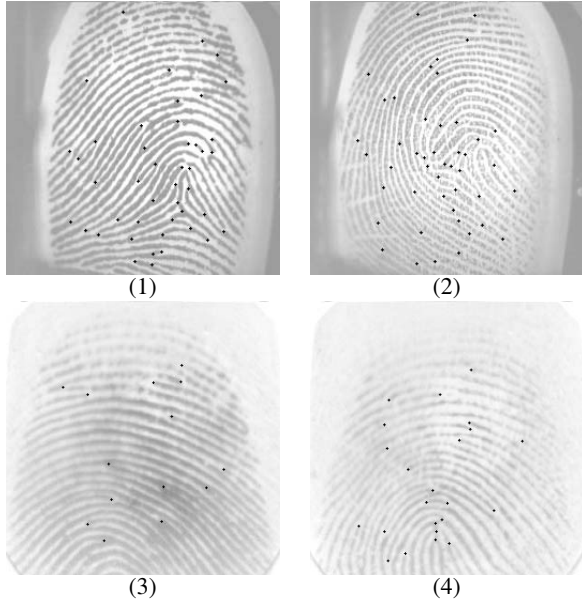


**Fig. 3.** Ground truth minutiae marked over four of the fingerprint images used in experiments.

the final curvature image of the fingerprint by selecting blocks, of  $16 \times 16$  pixels, from different candidates, in accordance to the criterion (14). Finally, the sign of the final curvature image is used to distinguish between the ridge and valley regions of the fingerprint.

We evaluated the proposed algorithm based on its ability to preserve the genuine minutia details and remove false minutiae from the fingerprint image. For comparison we implemented also the enhancement algorithm described in [8]. Each algorithm was combined with the same minutiae extraction module, and the performance have been measured based on the numbers of missing and spurious minutiae after processing, using [4]:

$$\begin{aligned} \text{Sensitivity} &= 1 - \frac{\text{Missing minutiae}}{\text{Ground truth minutiae}} \\ \text{Specificity} &= 1 - \frac{\text{Spurious minutiae}}{\text{Ground truth minutiae}} \end{aligned} \quad (15)$$

A number of 20 fingerprint images have been used in our experiments. The “ground truth” consists of the fingerprint minutiae manually detected in each fingerprint image, as exemplified in Fig. 3. The results obtained for the four images shown in Fig. 3, are presented in Table 1. Overall, for all images used in experiment, a lower number of missing minutiae was achieved with this enhancement algorithm than with the algorithm described in [8]. This is also reflected by the average sensitivity which was 87% when this enhancement algorithm was used, and 70% when the other enhancement method was used. On the other hand, method [8] achieves a slightly higher average specificity (74%) than the present enhancement algorithm (72%).

## 5. CONCLUSIONS

In this paper we introduced a method of fingerprint image enhancement that relies on the sign of second directional derivative of the

Image	Ground truth minutiae	Enhancement method	Missing minutiae	Spurious minutiae
1	45	a / b	<b>0</b> / 4	5 / <b>3</b>
2	46	a / b	<b>12</b> / 15	7 / <b>5</b>
3	14	a / b	<b>0</b> / 3	1 / <b>2</b>
4	23	a / b	<b>3</b> / 5	<b>18</b> / 20

**Table 1.** Performance of minutiae detection algorithm applied to fingerprint images enhanced with different enhancement methods: (a) is the proposed method; and (b) is the method in [8].

digital image. A polynomial facet model was employed to estimate the derivatives of the discrete intensity surface of the image in each image pixel. The approximation accuracy achieved by the facet model determines the minimum size of those image details that are preserved by the operation. The most important image features that should be preserved are fingerprint minutiae and their sizes are in the range of local ridge period. Thus, we proposed a criterion for the selection of the approximation accuracy such that to ensure the preservation of image details whose sizes are comparable with the ridge period. The proposed algorithm was evaluated on several fingerprint images, and compared against another fingerprint enhancement algorithm proposed in the literature.

## 6. REFERENCES

- [1] Lawrence O’Gorman, “Fingerprint verification,” in *Biometrics - Personal Identification in Networked Society*, A. K. Jain, R. Bolle, and S. Pankanti, Eds., pp. 43–64. Kluwer Academic, 1999.
- [2] Nalini K. Ratha, Shaoyun Chen, and Anil K. Jain, “Adaptive flow orientation-based feature extraction in fingerprint images,” *Pattern Recognition*, vol. 28, no. 11, pp. 1657–1672, 1995.
- [3] Anil K. Jain, Lin Hong, Sharath Pankanti, and Ruud Bolle, “An identity-authentication system using fingerprints,” *Proceedings of the IEEE*, vol. 85, no. 9, pp. 1365–1388, 1997.
- [4] B. G. Sherlock, D. M. Monro, and K. Millard, “Fingerprint enhancement by directional Fourier filtering,” *IEE Proc.-Vis. Image Signal Processing*, vol. 141, no. 2, pp. 87–94, 1994.
- [5] A. J. Willis and L. Myers, “A cost-effective fingerprint recognition system for use with low-quality prints and damaged fingertips,” *Pattern Recognition*, vol. 34, no. 2, pp. 255–270, 2001.
- [6] R. M. Haralick, “Digital step edges from zero crossing of second directional derivatives,” *IEEE Trans. on Pattern Analysis and Machine Intelligence*, vol. PAMI-6, no. 1, pp. 58–68, 1984.
- [7] Marius Tico and Pauli Kuosmanen, “Weighted least squares method for the approximation of directional derivatives,” in *Proc. of the IEEE International Conference on Acoustics, Speech, and Signal Processing (ICASSP)*, 2001, vol. 3, pp. 1681–1684.
- [8] Marius Tico, Vesa Onnia, and Pauli Kuosmanen, “Fingerprint image enhancement based on second directional derivative of the digital image,” *EURASIP Journal on Applied Signal Processing*, , no. 10, pp. 1135–1144, 2002.